



# Herbicide symptomology and the mechanism of action of methiozolin

Chad Brabham<sup>1</sup> , Philipp Johnen<sup>2</sup> , Janneke Hendriks<sup>3</sup>, Michael Betz<sup>4</sup>, Alexandra Zimmermann<sup>2</sup>, Jarrad Gollihue<sup>5</sup>, William Serson<sup>6</sup>, Chase Kempinski<sup>7</sup> and Michael Barrett<sup>8</sup>

## Research Article

**Cite this article:** Brabham C, Johnen P, Hendriks J, Betz M, Zimmermann A, Gollihue J, Serson W, Kempinski C, Barrett M (2021) Herbicide symptomology and the mechanism of action of methiozolin. *Weed Sci.* **69**: 18–30. doi: [10.1017/wsc.2020.87](https://doi.org/10.1017/wsc.2020.87)

Received: 18 February 2019  
Revised: 28 June 2019  
Accepted: 18 November 2020  
First published online: 3 December 2020

### Associate Editor:

Franck E. Dayan, Colorado State University

### Keywords:

Annual bluegrass (*Poa annua* L.); cellulose biosynthesis inhibitors (CBI); cinmethylin; fatty-acid synthesis inhibition; fatty-acid thioesterase (FAT); tyrosine aminotransferase (TAT)

### Author for correspondence:

Michael Barrett, Department of Plant and Soil Sciences, University of Kentucky, Lexington, KY 40546-0312. (Email: [mbarrett@uky.edu](mailto:mbarrett@uky.edu))

<sup>1</sup>Former Graduate Student, Department of Horticulture, University of Kentucky, Lexington, KY, USA; current: Stine Research Center, FMC Corporation, Elkton, Delaware USA; <sup>2</sup>Team Leader, BASF SE, Limburgerhof, Germany; <sup>3</sup>Senior Scientist, BASF Metabolome Solutions GmbH, Berlin, Germany; <sup>4</sup>Team Leader, BASF SE, Ludwigshafen am Rhein, Germany; <sup>5</sup>Graduate Student, Department of Horticulture, University of Kentucky, Lexington, KY, USA; <sup>6</sup>Assistant Professor, Department of Biology, Ave Maria University, Ave Maria, FL, USA; <sup>7</sup>Former Graduate Student, Department of Pharmaceutical Science Lexington, KY, USA and <sup>8</sup>Professor, Department of Plant and Soil Sciences, University of Kentucky, Lexington, KY, USA

## Abstract

Methiozolin is a new herbicide with an unknown mechanism of action (MOA) for control of annual bluegrass (*Poa annua* L.) in several warm- and cool-season turfgrasses. In the literature, methiozolin was proposed to be a pigment inhibitor via inhibition of tyrosine aminotransferases (TATs) or a cellulose biosynthesis inhibitor (CBI). Here, exploratory research was conducted to characterize the herbicide symptomology and MOA of methiozolin. *Arabidopsis* (*Arabidopsis thaliana* L.) and *P. annua* exhibited a similar level of susceptibility to methiozolin, and arrest of meristematic growth was the most characteristic symptomology. For example, methiozolin inhibited *A. thaliana* root growth (GR<sub>50</sub> 8 nM) and shoot emergence (GR<sub>80</sub> ~50 nM), and apical meristem growth was completely arrested at rates greater than 500 nM. We concluded that methiozolin was neither a TAT nor a CBI inhibitor. Methiozolin had a minor effect on chlorophyll and alpha-tocopherol content in treated seedlings (<500 nM), and supplements in the proposed TAT pathway could not lessen phytotoxicity. Examination of microscopic images of roots revealed that methiozolin-treated (100 nM) and untreated seedlings had similar root cell lengths. Thus, methiozolin inhibits cell proliferation and not elongation from meristematic tissue. Subsequently, we suspected methiozolin was an inhibitor of the mevalonic acid (MVA) pathway, because its herbicidal symptomologies were nearly indistinguishable from those caused by lovastatin. However, methiozolin did not inhibit phytosterol production, and MVA pathway metabolites did not rescue treated seedlings. Further experiments showed that methiozolin produced a physiological profile very similar to cinmethylin across a number of assays, a known inhibitor of fatty-acid synthesis through inhibition of thioesterases (FATs). Experiments with lesser duckweed (*Lemna aequinoctialis* Welw.; syn. *Lemna paucicostata* Hegelm.) showed that methiozolin also reduced fatty-acid content in *Lemna* with a profile similar, but not identical, to cinmethylin. However, there was no difference in fatty-acid content between treated (1 μM) and untreated *A. thaliana* seedlings. Methiozolin also bound to both *A. thaliana* and *L. aequinoctialis* FATs in vitro. Modeling suggested that methiozolin and cinmethylin have comparable and overlapping FAT binding sites. While there was a discrepancy in the effect of methiozolin on fatty-acid content between *L. aequinoctialis* and *A. thaliana*, the overall evidence indicates that methiozolin is a FAT inhibitor and acts in a similar manner as cinmethylin.

## Introduction

Methiozolin [MRC-101, 5(2,6-difluorobenzyl)oxymethyl-5-methyl-3,3(3-methylthiophen-2-yl)-1,2-isoxazoline] is a herbicide in the isoxaline chemical family originally considered for weed management in rice (*Oryza sativa* L.) (Hwang et al. 2005; Ryu et al. 2002). It was originally registered in Korea and Japan for use in turfgrass (Koo et al. 2014) and was registered for that use in 2019 in the United States (Anonymous 2019b). A primary weed target for methiozolin is *P. annua* in established creeping bentgrass (*Agrostis stolonifera* L.) and other cool- and warm-season turfgrasses (Askew and McNulty 2014; Brosnan et al. 2013; Flessner et al. 2013; Koo et al. 2014; Venner 2015; Yu and McCullough 2014). However, certain *Agrostis* spp. and cultivars are sensitive to methiozolin (Hoisington et al. 2014).

Methiozolin is a lipophilic herbicide (logK<sub>ow</sub> 3.9) that is readily absorbed by roots and shoots but is not phloem mobile and has little to moderate translocation in the xylem (Flessner et al. 2013; McCullough et al. 2013; Yu and McCullough 2014). The variation in methiozolin

sensitivity found within and among established turfgrasses and *P. annua* was partially attributed to differences in absorption and translocation, but not metabolism (Flessner et al. 2013; McCullough et al. 2013; Yu and McCullough 2014). Target-site sensitivity or growth phenology differences were also proposed as alternative tolerance mechanisms.

Two possible mechanisms of action (MOAs) have been proposed for methiozolin. Lee et al. (2007) proposed methiozolin either directly or indirectly inhibits cell wall biosynthesis. The MOA of cellulose biosynthesis inhibitors (CBIs), while not completely understood, causes a decrease in the incorporation of glucose into expanding cellulose microfibrils (Brabham and Debolt 2012). For a herbicide to be classified as a CBI, it must meet three criteria: (1) treated seedlings are phenotypically stunted and rapidly expanding tissue appears swollen, (2) cellulose synthesis is rapidly (within 2 h after treatment [HAT]) inhibited, and (3) cellulose content is reduced in a dose-dependent manner (Brabham and Debolt 2012; Sabha and Vaughn 1999). Lee et al. (2007) found that 1  $\mu\text{M}$  methiozolin caused corn (*Zea mays* L.) root growth to be nearly stopped 6 HAT. The incorporation of [ $^{14}\text{C}$ ]glucose into the cellulose and hemicellulose fractions of the corn roots was severely inhibited at 12 and 24 HAT, but inhibition was variable at earlier time points. Although not a rapid inhibition, the inhibition of glucose incorporation into cellulose is consistent with a CBI MOA. In addition, while both the shoot and root growth of barnyardgrass [*Echinochloa crus-galli* (L.) P. Beauv.] seedlings were inhibited by methiozolin, the observed symptomologies were dissimilar to those of the known CBI dichlobenil. Taken together, the results of Lee et al. (2007) offer little support for methiozolin acting as a CBI.

Alternatively, Grossmann et al. (2012), based on data from metabolomic profiling and metabolite supplementation of methiozolin-treated lesser duckweed (*Lemna aequinoctialis* Welw.; syn. *Lemna paucicostata* Hegelm.), suggested that methiozolin prevents formation of plastoquinone and tocopherol through inhibition of tyrosine aminotransferases (TATs; EC 2.6.1.5). TATs are responsible for the conversion of tyrosine to 4-hydroxyphenyl-pyruvate and ultimately homogentisate. Homogentisate is an essential branch-point metabolite for both the prenylquinone and tocopherol pathways (DellaPenna and Pogson 2006). Functionally, TATs are directly upstream of the enzymatic target of 4-hydroxyphenyl-pyruvate-dioxygenase (HPPD) inhibitors. Thus, the inhibitory mechanism of methiozolin would be essentially similar to that of HPPD-inhibiting herbicides. Susceptible plants treated with HPPD inhibitors lack pigmentation or become “bleached” in new tissue, which is followed by necrosis (Shaner 2014). Consistent with TAT inhibition, Grossmann et al. (2012) observed photobleaching in newly formed fronds of *L. aequinoctialis* within 72 h of methiozolin treatment. However, photobleached tissue later became “greenish with a touch of brown,” and the meristematic tissue was necrotic. Methiozolin was also shown to inhibit *Arabidopsis* (*Arabidopsis thaliana* L.) TAT7 activity in vitro. However, the inhibition only occurred at extremely high methiozolin concentrations ( $\geq 62 \mu\text{M}$ ). Grossmann et al., (2012) hypothesized that another TAT(s) or that TATs in grass species would be inhibited at lower methiozolin concentrations.

The studies described in this paper were undertaken to investigate the MOA of methiozolin in more detail. Experiments were conducted at the University of Kentucky and at BASF. In the paper, we exclude several physiological processes as the target site of methiozolin and present evidence that methiozolin is a fatty acid thioesterase (FAT) inhibitor.

## Materials and Methods

### Plant Growth Conditions and Measurements

*Arabidopsis thaliana* (ecotype Columbia) and *P. annua* grass seeds were surface sterilized for 15 min in Eppendorf tubes with 30% household bleach and subsequently washed three times with sterilized distilled water and kept at 4 C for 2 d. Seeds were placed on agar plates placed vertically in growth chambers (22 C and a 16-h photoperiod). Agar media was made by autoclaving a 1-L solution containing 2.25 g of Murashige and Skoog (MS) Basal Salt Mixture (Phyto Technology Laboratories, Shawnee Mission, KS), 0.6 g of 2-(*N*-Morpholino)-ethanesulfuric acid (MES), and 11 g of agar. The pH of the solution was 5.7 to 5.8. Agar plates were made with or without methiozolin by pouring 40 ml of autoclaved MS-agar media into a 50-ml Falcon tube, which was then capped and shaken, and the solution was poured directly into plates and allowed to solidify. Compounds were added to the tubes before capping. The plates used in all experiments were a sterile square petri dish with grids (100 mm by 100 mm by 15 mm; Simport). Methiozolin (purity 99.71%) was supplied by the Moghu Research Center. A 100 mM stock solution was made by dissolving methiozolin in dimethyl sulfoxide (DMSO), and this was subsequently diluted with DMSO to obtain appropriate concentrations. Concentrations of DMSO above 0.1% in agar plates are injurious to *A. thaliana*, and thus no more than 40  $\mu\text{l}$  of the methiozolin solution was added to obtain the desired methiozolin rates. DMSO (0.05% v/v) alone was included in the untreated control in all experiments. *Arabidopsis thaliana* seeds germinate very quickly, and the first day after plating was considered 1 d after treatment (DAT). *Poa annua* seed was pre-germinated on water saturated filter paper in petri dishes before being transferred to the treatment plates. *Poa annua* that had a protruding radicle <1 mm were selected and transferred. For *A. thaliana*, each plate had two rows of seeds, and each row had roughly 10 seeds. For *P. annua*, only one row of 12 pre-germinated seeds was used.

Root and hypocotyl lengths were measured at 7 DAT. Plates were photographed, and ImageJ (Schneider et al. 2012) was used to measure root length. The grid pattern on square plates used in these experiments had an area of 1  $\text{cm}^2$ . This allowed us to convert pixel number into centimeters. Lengths are expressed as a percentage of the untreated control. At 14 DAT, shoot tissue from four randomly sampled plants was harvested, and fresh weight was measured. The four-plant sample was considered a replication, and three replications were taken from each treatment plate. To determine the effect of methiozolin on hypocotyl growth, plates were exposed to light for 2 h, wrapped in aluminum foil, and then placed vertically into the growth chamber.

### Effect of Methiozolin on Plant Growth

#### Dose-Response Experiments

*Arabidopsis thaliana* and *P. annua* seedlings were grown on agar plates with different concentrations (0, 10, 25, 37, 50, 75, 100, 500 nM, or 1  $\mu\text{M}$ ) of methiozolin as described earlier. In the case of the dark-grown *A. thaliana* (hypocotyl expansion determination) experiment, the methiozolin concentrations used were: 0, 1, 5, 10, 25, 50, or 100  $\mu\text{M}$ . A minimum of 10 plants were measured per treatment plate, and treatment plates were replicated three times in time. Dose-response curves were generated in R using the DRC package (Ritz et al. 2015).

### Chlorophyll Measurement

To determine whether methiozolin causes a loss in chlorophyll content, *A. thaliana* seedlings were treated with methiozolin (0, 5 nM, 50 nM, 500 nM, 5  $\mu$ M, and 50  $\mu$ M) as described earlier. At 7 and 14 DAT, shoot tissue was harvested, weighed, placed into Eppendorf tubes, frozen in liquid nitrogen, and stored at  $-80$  C until being used for chlorophyll determinations. Chlorophyll was extracted as follows (Ritchie 2006): shoot tissue was homogenized with a micropestle in Eppendorf tubes with 300  $\mu$ l of extraction buffer (1:1:1 ratio of 90% v/v acetone:methanol:ethanol). This step was done under dim light. Tubes were centrifuged for 5 min at  $2,300 \times g$ . Afterward, 50  $\mu$ l of the supernatant was combined with 950  $\mu$ l of ethanol. Chlorophyll *a* and *b* were measured spectrophotometrically at 665 nm and 649 nm, respectively. Absorbance values were used to calculate chlorophyll content per milligram using Equations 1–3 (Ritchie 2006):

$$\text{Chlorophyll } a = 13.7 \times A_{665} - (5.76 \times A_{649}) \quad [1]$$

$$\text{Chlorophyll } b = -7.6 \times A_{665} + (25.8 \times A_{649}) \quad [2]$$

$$\text{Total Chlorophyll} = \text{Chlorophyll } a + \text{Chlorophyll } b \quad [3]$$

### Root Cell Length Measurement

*Arabidopsis thaliana* seedlings expressing Plasma membrane Intrinsic Protein 2:Red Fluorescent Protein (PIP2:RFP) were grown on agar plates supplemented with DMSO (0.05% v/v), methiozolin (100 nM), or indaziflam (2 nM) as described earlier. Fluorescence from PIP2:RFP colocalizes with the plasma membrane and can be used to outline cells (Cutler et al. 2000). Images of roots from 3-d-old PIP2:RFP plants were taken on an Olympus IX83 confocal microscope using a 40 $\times$  water objective. Images of roots from 10 plants per treatment plate were taken, and the experiment was repeated. Six cells from the zone of elongation and maturation were measured per plant using ImageJ (National Institutes of Health, Bethesda, MD 20892). Scale bars acquired during imaging were used to convert pixels to millimeter lengths.

### Metabolite Supplementation Studies

To see whether methiozolin phytotoxicity could be reversed by metabolite supplementation, *A. thaliana* seedlings were grown on agar plates with methiozolin (5 or 50 nM) with or without supplements. To test whether methiozolin is a TAT-inhibiting herbicide, agar plates were supplemented with 10  $\mu$ M chorismate, tyrosine + phenylalanine, 4-hydroxyphenyl-pyruvate, or homogentisate. In addition, mesotrione (20 nM) was included as a positive control for supplements' efficacy. For the mevalonate supplementation assay, the positive control, lovastatin (1  $\mu$ M; ([1S-[1 $\alpha$ (R\*),3 $\alpha$ ,7 $\beta$ ,8 $\beta$ (2 S\*,4 S\*),8 $\alpha$ ]])-1,2,3,7,8,8a-hexahydro-3,7-dimethyl-8-[2-(tetrahydro-4-hydroxy-6-oxo-2 H-pyran-2-yl)ethyl]-1-naphthalenyl 2-methylbutanoate)), methiozolin, or DMSO (0.05% v/v) were supplemented with 20  $\mu$ M of *trans*, *trans*-farnesol, or squalene. Lovastatin, farnesol, and squalene were kindly provided by the laboratory of Joseph Chappell at the University of Kentucky Department College of Pharmacy and were diluted in DMSO, methanol, and acetone, respectively. Otherwise, all supplements were from Sigma and were dissolved in water. Root lengths were measured at 7 DAT and shoot fresh weights at 14 DAT as described earlier. The study was repeated three times in time.

### Measurement of $\alpha$ -Tocopherol

*Arabidopsis thaliana* plants were grown on agar plates containing DMSO or methiozolin (5, 50, or 500 nM) as described earlier. Shoot tissue was harvested at 7 and 14 DAT, weighed, placed in Eppendorf tubes, frozen in liquid nitrogen, and stored at  $-80$  C until used. Tocopherols were extracted and quantified using the official AOCS method (Xu 2002; modified for Eppendorf tube volume). Briefly, tissue was ground in the Eppendorf tube using a micropestle with 500  $\mu$ l of 90% (v/v) ethanol and 50  $\mu$ l 800 g L $^{-1}$  potassium hydroxide. Samples were placed in a 70 C water bath for 30 min followed 5 min in an ice bath. Then, 300  $\mu$ l of water and 500  $\mu$ l of hexane were added, and the samples were vortexed and centrifuged at  $1,000 \times g$  for 10 min. The nonaqueous (upper) phase was removed and retained. An additional 500  $\mu$ l of hexane was added to the remaining aqueous phase, and the procedure was repeated. The collected nonaqueous phases were combined, dried under nitrogen flow, dissolved in 1 ml of methanol, and filtered (0.4  $\mu$ m). Samples (200  $\mu$ l) were injected into a high-performance liquid chromatography column equipped with a C18 column (Inertsil ODS-3, Millipore-Sigma, St Louis, MO 63178). The flow rate was 1 ml min $^{-1}$  and the mobile phase was 50:46:4 v/v/v methanol:acetonitrile:methylene chloride. UV fluorescence was measured at 295 nm. Calibration curves were generated and used to determine  $\alpha$ -tocopherol concentrations, and tocopherinol (100  $\mu$ M) was added as an internal standard before sample extraction. Two subsamples were taken per treatment plate, and treatment plates were replicated in time ( $n = 6$ ).

### Major Phytosterol Measurement

*Arabidopsis thaliana* plants were grown on agar plates containing DMSO or methiozolin (1  $\mu$ M) as described earlier. At 72 HAT, whole seedlings ( $\sim 20$  mg fresh weight) were placed in Eppendorf tubes, frozen in liquid nitrogen, and stored at  $-80$  C until used. Treatment plates were repeated three times in time. To quantify the change in major plant sterol content,  $\beta$ -sitosterol, stigmasterol, and campesterol levels were determined by grinding  $\sim 20$  mg of plant tissue in liquid nitrogen, which was followed by saponification and extraction as described by Jiang et al. (2016). Briefly, 5 ml of ethanol:33% potassium hydroxide 94:6) and 250  $\mu$ l of 200 g L $^{-1}$  ascorbic acid (made fresh) was added to the homogenized tissue. The mixture was vortexed and incubated at 50 C for 1 h and then cooled on ice for 10 min. Next, 7.5 ml of water and 7.5 ml of hexane were added, and sterols were extracted by shaking at room temperature for  $\sim 20$  min. The phases were separated by briefly centrifuging, and the hexane (upper) phase was collected. The sample was partitioned once more with 7.5 ml of hexane, and the hexane phases were pooled. The hexane was dried to completion with nitrogen gas, and samples were derivatized using a 1:1 mixture of pyridine and MSTFA (N-Methyl-N-trimethylsilyltrifluoroacetamide) + 1% TMCS (2, 2, 2-Trifluoro-N-methyl-N-(trimethylsilyl)-acetamide, Chlorotrimethylsilane; Thermo-Fisher, Grand Island, NY 14072) at 50 C for 1 h (total volume 50  $\mu$ l). Samples were analyzed on an Agilent 7890 gas chromatography system (Agilent Technologies, Santa Clara, CA 95050; HP-5MS column, 30 m by 0.25 mm, 0.25  $\mu$ m film, 250 C inlet temperature; oven temperature was 200 C for 1 min, then increased at 10 C min $^{-1}$  to 270 C, then increased at 3 C min $^{-1}$  to 320C, then held at 320 C for 10 min; 0.9 ml min $^{-1}$  He flow rate) connected to a mass spectrometer (run in positive ionization mode, 70 eV, scanning 50 to 500 amu).



## Physiological Assays

All physiological assays were carried out as previously described (Grossmann 2005; Grossmann et al. 2012). Assays performed included cell suspensions of heterotrophic false baby's breath (*Galium mollugo* L.), photoautotrophic green algae [*Scenedesmus obliquus* (Turpin) Kützing], *L. aequinoctialis* plants, and germinating gardencress pepperweed (*Lepidium sativum* L.) seedlings. Effects on the Hill reaction in isolated wheat (*Triticum aestivum* L.) chloroplasts, carbon assimilation in *G. mollugo* plants, O<sub>2</sub> consumption in heterotrophic *G. mollugo* cell suspensions, uncoupler activity and accumulation of reactive oxygen species (ROS) in *L. aequinoctialis* root tissue, and toluidine-blue staining of *L. sativum* hypocotyls for the detection of inhibition of very-long-chain fatty-acid (VLCFA) synthesis were also tested. Additionally, *A. thaliana* seedling morphology, *L. aequinoctialis* chlorophyll fluorescence, and adenosine triphosphate (ATP) content of *L. aequinoctialis* were evaluated. In brief, for the *A. thaliana* assay, sterilized seeds (MC24 ecotype) were stratified overnight at 4 C in 48-well plates containing 250 µl half-strength MS including Gamborg's B5 vitamins (Millipore-Sigma) containing 2.5 µl of acetone (as solvent control) or 2.5 µl of the respective compound, resulting in the following concentrations 0.001, 0.01, and 0.1 mM. The 48-well plates were sealed with micropore tape and grown for 7 d in constant light at 22 C under 75% humidity. Growth inhibition and symptoms were evaluated manually. *Lemna aequinoctialis* growth was carried out as described in Grossmann (2005). Effects on chlorophyll fluorescence (fluorescence quantum yield, Y(II)) were measured after 24 h compound treatment using an Imaging Pulse-Amplitude-Modulation (PAM) M-Series system (Walz, Effeltrich, Germany). ATP content was measured with the ATP Determination Kit (A22066, Thermo Fisher Scientific, Grand Island, NY 14072) according to the manufacturer's instructions using *L. aequinoctialis* extracts. Results were normalized to fresh weight.

## Measurement of Fatty Acids

Preparation, treatment, and sampling of *L. aequinoctialis* plants for the measurement of free fatty acids (FFAs) was performed as described in Grossmann et al. (2010). Samples were taken at 6, 24, and 48 HAT, and three independent replicates were individually sampled per treatment and time point. Controls were treated with the same final concentration of acetone and sampled at each time point. Measurement and analysis of the samples were performed as described in Campe et al. (2018).

For measurement of fatty acids in *A. thaliana* plants were grown in liquid culture (MS media without agar) in the presence or absence of methiozolin (1 µM). Whole seedlings were harvested at 72 HAT, dried, weighed, placed in Eppendorf tubes, frozen in liquid nitrogen, and stored at -80 C until used. Treatments were repeated three times over time. Seed coats were removed before weighing. Fatty acids were extracted using a modified Bligh and Dyer technique (Iverson et al. 2001). Briefly, ~20 mg of tissue was added to an Eppendorf tube and mixed in a solution of 320 µl ice-cold chloroform together with 640 µl of ice-cold of methanol containing butylated hydroxytoluene (50 µg ml<sup>-1</sup>) with occasional vortexing for 20 min. Afterward, 300 µl of water was added, and the sample was centrifuged for 5 min at 2,000 × g. All of the upper (aqueous) phase was removed, and both phases were retained. The aqueous phase was centrifuged again to recover the residual organic phase. Finally, the aqueous phase was discarded. The combined organic phases were dried under a stream of nitrogen and stored at -80 C until used. For gas chromatography-flame ionization detector

(GC-FID) analysis, 0.5 M sodium methoxide (1 ml) was added to each Eppendorf tube, and the tube was shaken for 10 min. Afterward, 1 ml of iso-octane containing 0.001% butylated hydroxytoluene (BHT) was added. Then, 200 µl from the upper layer was extracted and transferred to a vial that already contained 1 ml of iso-octane. Samples were run on a Varian CP-3800 gas chromatograph (Varian, Palo Alto, CA) equipped with a with an Agilent Varian 25 m by 0.25 mm ID fused silica column (Chrompack, CP=Select CB for Fatty Acid Methyl Esters [FAME]), with a film thickness of 0.25 µm. The temperature program ran from 90 C to 250 C, with 25 C ramp rate for an 8-min runtime with a constant column flow mode of 0.9 ml min<sup>-1</sup> utilizing a splitless injection. Quantification was performed using an FID, and peaks were quantified using Star Chromatography Workstation v. 6.00 (Agilent Technologies). Peak area for each fatty acid was measured and expressed as relative percentage of the total FAMES area.

## FAT Expression and Purification

Expression and purification of used FAT proteins were performed as described in Campe et al. (2018).

## Fluorescence-based Thermal Shift Assay (FTSA)

The protocol for this assay was modified and optimized from that of Layton and Hellinga (2010), as outlined in Campe et al. (2018).

## Molecular Modeling

The BASF internal X-ray structure for the cinmethylin-FAT A complex and the docking program GOLD (Jones et al. 1997) were used to generate methiozolin arrangements in the cinmethylin binding site. Local minimization of the highest-scoring pose using the Molecular Operating Environment (MOE v. 2019.01; Anonymous 2019a) resulted in the binding arrangement presented in this paper.

## Statistical Analysis

Before analysis, all data were checked for basic ANOVA assumptions. There were no run by treatment interactions in any experiment, so data were combined over experimental runs. Means were separated using a Tukey's or Dunnett's test and were considered significantly different at an alpha value of <0.05. Statistical analysis of FFA in *L. aequinoctialis* was performed as described in Campe et al. (2018).

## Results and Discussion

### Effect of Methiozolin on Plant Growth

Methiozolin is phytotoxic to a number of grass and sedge weeds (Grossmann et al., 2012; Hwang et al. 2005; Lee et al. 2007; Ryu et al. 2002), but its activity on broadleaves is not as well documented. In this study, *A. thaliana*, *P. annua* (Figure 1A–D), and soybean [*Glycine max* (L.) Merr.] (data not shown) responded similarly to methiozolin, with growth being severely inhibited at rates exceeding 100 nM. Our rate range is consistent with rates used by other authors to inhibit growth in grass species and *L. aequinoctialis* (Grossman et al. 2012; Lee et al. 2007; Venner 2015). In all species, meristematic growth was more sensitive to methiozolin than cotyledon tissue (i.e., the hypocotyl of dicots or coleoptiles of grasses). For light-grown plants, methiozolin GR<sub>50</sub> values were 8 nM for *A. thaliana* root growth, 12 nM for *P. annua* root growth, and 26 nM for *P. annua* shoots. In contrast, dark-grown plants required

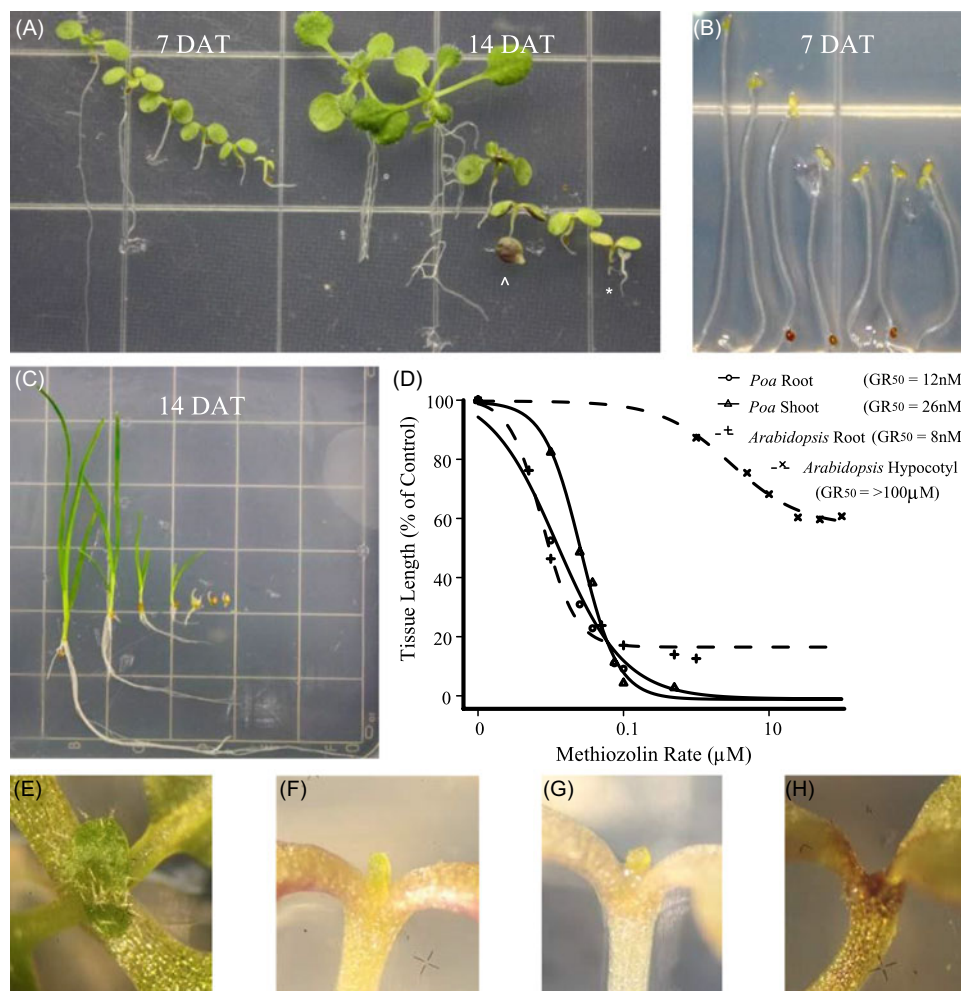


**Figure 1.** Photographs and a graph showing the symptomology and dose responses of methiozolin-treated *Arabidopsis thaliana* and *Poa annua* seedlings at 7 and 14 d after treatment (DAT). (A) Photograph showing symptomology of *A. thaliana* seedlings treated with methiozolin at 7 and 14 DAT. Within a time point, the rates from left to right are: 0, 5 nM, 50 nM, 500 nM, 5 μM, 50 μM. Caret (^) highlights the purpling on the underside of cotyledons at 500 nM. Asterisk (\*): These two plants exhibit the types of symptoms seen at 50 μM at 14 DAT. (B) Photograph of *A. thaliana* seedling hypocotyl growth in the dark at 7 DAT and treated with methiozolin at (left to right) 0, 1, 5, 10, 25, 50, and 100 μM. (C) Photograph of root and shoot growth of light-grown *P. annua* seedlings at 14 DAT. The seedlings were treated with (from left to right) 0, 10 nM, 25 nM, 37.5 nM, 75 nM, 100 nM, and 500 nM methiozolin (D) Methiozolin dose response curves for *A. thaliana* and *P. annua* and the calculated rate that reduces root, shoot, or hypocotyl growth by 50% (GR<sub>50</sub>). (E–H) Close-up images of the apical meristems from *A. thaliana* plants treated with (E) dimethyl sulfoxide (DMSO) control, (F) 500 nM, (G) 5 μM, and (H) 50 μM methiozolin at 14 DAT. Scale bars: (A–C) 0.2 cm; (E–H) 0.2 mm.

approximately a 1,000-fold increase in methiozolin concentration before methiozolin inhibited elongation of *A. thaliana* hypocotyls (Figure 1B and D). At the highest tested rate, 100 μM, methiozolin did not inhibit hypocotyl elongation more than 30%, so a GR<sub>50</sub> could not be determined. Seedlings treated with >1 μM methiozolin exhibited abnormal skotomorphogenesis, mainly loss of the apical hook and cotyledon expansion (Figure 1B).

Methiozolin injury symptomology observed in *A. thaliana* seedlings was primarily a shortening of the primary root length with no apparent swelling at 7 DAT (Figure 1A). At 14 DAT, lateral roots were present in untreated plants, partially stunted in plants treated with 5 nM, and absent in seedlings treated with rates above 50 nM. Lateral roots were present in seedlings treated with 50 nM methiozolin, but they did not elongate, resulting in knotty root phenotype. Shoot tissue and the apical meristem of light-grown *A. thaliana* treated seedlings also exhibited unique concentration-dependent symptomologies (Figure 1A). At 7 DAT, emergence of true leaves was increasingly delayed at rates above 10 nM and was completely arrested above 500 nM. Chlorophyll content of *A. thaliana* seedlings at 7 DAT was only reduced (41%) at the

highest rate tested (50 μM) (Table 1). At 14 DAT, methiozolin significantly reduced chlorophyll content at all concentrations above 5 nM to a maximum of 82%. At rates between 50 nM and 5 μM, shoot tissue and, especially, the abaxial side of cotyledons developed a purple tinge (^ in Figure 1A), and as rates exceeded 500 nM, plants were more chlorotic. A bleached seedling morphology was observed at the highest rate tested (50 μM), but only one-third of the seedlings exhibited this response (Figure 1A, \* marks the two bleached seedlings observed on the 50 μM plates at 14 DAT). The apical meristem of seedlings treated with 500 nM, while severely chlorotic, still appeared to be meristem-like (Figure 1F). However, as the methiozolin rate increased to 5 μM, the meristem appeared to be an undifferentiated mass of chlorotic cells (Figure 1G) and at 50 μM was necrotic (Figure 1H).

#### Is Methiozolin a CBI? Root Cell Length Measurement

To determine whether methiozolin-treated seedlings exhibited symptoms characteristic of CBI inhibitors, such as loss of anisotropic cell expansion, we examined and measured the length

**Table 1.** Effect of increasing methiozolin rate on chlorophyll content in the shoot tissue of *Arabidopsis thaliana* seedlings at 7 and 14 d after treatment (DAT).

| Rate   | Chlorophyll content |                            |        |    |
|--------|---------------------|----------------------------|--------|----|
|        | 7 DAT               |                            | 14 DAT |    |
| nM     |                     | -% of Control <sup>a</sup> |        |    |
| 0      | 100                 | AB                         | 100    | A  |
| 5      | 91                  | AB                         | 100    | A  |
| 50     | 102                 | A                          | 70     | B  |
| 500    | 94                  | AB                         | 56     | BC |
| 5,000  | 86                  | B                          | 42     | C  |
| 50,000 | 59                  | C                          | 18     | D  |

<sup>a</sup>Means in a column not followed by the same letter are significantly different ( $P < 0.05$ ).

of root cells of *A. thaliana* seedlings treated with or without methiozolin at 100 nM. A treatment with indaziflam (2 nM), a known CBI (Brabham et al. 2014), was included as a positive control. This indaziflam rate inhibits *A. thaliana* root growth comparable to 100 nM methiozolin based on root GR<sub>50</sub> values (Brabham et al. 2014). To measure root cell lengths, we used confocal microscopy to capture fluorescence from treated transgenic *A. thaliana* plants expressing a red fluorescently (RFP) labeled aquaporin called plasma membrane intrinsic protein 2 (PIP2). This protein is plasma membrane bound and can be used to outline the plasma membrane of cells and thus the length of cell. In these images, there was no apparent change in root cell morphology between the control plants (Figure 2A) and those treated with methiozolin (Figure 2C). In contrast, the root cells from plants treated with indaziflam (Figure 2B) showed swelling and loss of anisotropic growth as expected from treatment with a CBI. Methiozolin also did not significantly reduce the length of root cells in the treated zone after division at 3 DAT (Figure 2D). Indaziflam, meanwhile, reduced cell length by 65% compared with both methiozolin-treated and control plants. These results strongly indicate that methiozolin is not a direct inhibitor of cellulose biosynthesis.

### Is Methiozolin a TAT Inhibitor? Metabolite Supplementation Study

It was proposed that methiozolin prevents the conversion of tyrosine to 4-hydroxyphenyl-pyruvate (4-HPP) by inhibition of TATs (Grossmann et al. 2012). This, in turn, would inhibit homogentisate biosynthesis and the subsequent tocopherol and prenylquinone biosynthesis pathways. Thus, TAT inhibition would produce similar physiological effects as HPPD inhibition. Based on this, we conducted a metabolite complementation study to determine whether additions of chorismate, tyrosine + phenylalanine, 4-HPP, or homogentisate (all at 10  $\mu$ M) could lessen the phytotoxic effects of methiozolin. We used methiozolin concentrations of 5 and 50 nM, which approximate the GR<sub>50</sub> values for roots and shoots, respectively. Tyrosine was not applied alone, because it is involved in feedback inhibitory loops (Huang et al. 2010). In a preliminary experiment, we demonstrated that adding 10  $\mu$ M homogentisate could partially counteract mesotrione (20 nM, a known HPPD inhibitor) phytotoxicity to *A. thaliana* (Supplementary Figure 1). At 14 DAT, mesotrione alone, mesotrione plus 4-HPP, or mesotrione plus homogentisate reduced *A. thaliana* shoot weights by 89%, 77%, and 56%, respectively, in comparison to the control (data not shown).

The addition of chorismate or tyrosine plus phenylalanine slightly reduced (7% and 11%, respectively) methiozolin inhibition of root growth at 7 DAT compared with the control

(no supplementation, 41% inhibition of root growth) (Table 2). Neither 4-HPP nor homogentisate reduced the effect of methiozolin on root growth. None of the supplements reduced the effect of methiozolin on shoot growth at 14 DAT (Figure 3A; Table 2). If methiozolin was preventing the formation of homogentisate because of inhibition of the TAT responsible for 4-HPP biosynthesis, then addition of homogentisate should have at least reduced methiozolin toxicity, as it did for mesotrione.

### Is Methiozolin a TAT Inhibitor? $\alpha$ -Tocopherol Content

Another way to examine whether methiozolin is inhibiting TATs is to measure the level of metabolites downstream of 4-HPP or homogentisate biosynthesis in the prenylquinone or tocopherol pathways. We measured the  $\alpha$ -tocopherol content of *A. thaliana* seedlings treated with methiozolin at 5, 50, or 500 nM at 7 and 14 DAT (Figure 3B). The  $\alpha$ -tocopherol content in shoot tissue of untreated plants at 7 and 14 DAT averaged 3 to 4  $\mu$ g g<sup>-1</sup>. These *A. thaliana*  $\alpha$ -tocopherol levels are consistent with those previously reported for young plants growing under ideal conditions (Porfirova et al. 2002; Riewe et al. 2012). Methiozolin had no effect on  $\alpha$ -tocopherol content at 7 DAT and actually increased the levels 2.6-fold at 14 DAT in both the 50 and 500 nM treatments (Figure 3B). The increase in  $\alpha$ -tocopherol levels may be a response to the stress caused by methiozolin injury (Holländer-Czytko 2005; Porfirova et al. 2002). It certainly shows the formation of  $\alpha$ -tocopherol is not inhibited by methiozolin and, consequently, methiozolin is not a direct inhibitor of the TAT for 4-HPP synthesis.

### Is Methiozolin an Mevalonic Acid Biosynthesis Inhibitor? Comparison of Methiozolin Injury Symptoms to Those Produced by Lovastatin

A guilt by association approach was next used to generate leads for the MOA of methiozolin. To do this, we conducted an extensive search of the *A. thaliana* literature for chemicals and/or genetic mutations that produced symptomologies similar to those we observed with methiozolin. Using this approach, we identified inhibition of enzymes in the mevalonic acid (MVA) pathway as a potential methiozolin MOA. Specifically, methiozolin could be acting as a statin mimic (Kobayashi et al. 2007; Rodriguez-Concepcion et al. 2004; Soto et al. 2011; Suzuki et al. 2004). The MVA pathway produces cytosolic-available isoprenoid units required for synthesizing membrane-essential phytosterols and other important compounds (Vranova et al. 2013). Statins inhibit an early step in the MVA pathway by targeting 3-hydroxy-3-methyl-glutaryl-coenzyme A reductase (HMG-CoA reductase). This enzyme is responsible for the conversion of HMG-CoA to mevalonate (Istvan and Deisenhofer 2001; Vranova et al. 2013). We conducted a side-by-side dose-response experiment with methiozolin and lovastatin to compare their symptomologies (Figure 4A). At 7 and 14 DAT, symptoms exhibited by *A. thaliana* seedlings treated with methiozolin or lovastatin were nearly indistinguishable. One difference we did note was the presence of adventitious roots in seedlings treated with lower lovastatin rates but not in those treated with methiozolin. Regardless, the remarkable similarities between these two compounds warranted further study.

### Is Methiozolin an MVA Biosynthesis Inhibitor? Metabolite Supplementation Study

Assuming methiozolin inhibits an early step in the MVA pathway, we tried to overcome the phytotoxic effects of methiozolin by



**Table 2.** Effect of tyrosine aminotransferase (TAT) pathway metabolites on phytotoxic effects of methiozolin at 7 and 14 d after treatment (DAT).

| TAT pathway metabolite <sup>a</sup> | 7 DAT root length                      |      |    |                           | 14 DAT shoot weight |   |       |    |
|-------------------------------------|--|------|----|---------------------------|---------------------|---|-------|----|
|                                     | Methiozolin concentration <sup>b</sup> |      |    |                           |                     |   |       |    |
|                                     | 0                                      | 5 nM |    | % of Control <sup>c</sup> |                     | 0 | 50 nM |    |
| None                                | 100                                    | A    | 59 | B                         | 100                 | A | 19    | AB |
| Chorismate                          | 88                                     | B    | 66 | A                         | 114                 | A | 17    | B  |
| Tyrosine + phenylalanine            | 91                                     | B    | 70 | A                         | 97                  | A | 21    | A  |
| 4-Hydroxy phenylpyruvate            | 86                                     | B    | 58 | B                         | 104                 | A | 18    | AB |
| Homogentisate                       | 100                                    | A    | 64 | AB                        | 111                 | A | 21    | A  |

<sup>a</sup>All metabolites were added at 10  $\mu$ M.

<sup>b</sup>5 nM is the  $\sim$ GR<sub>50</sub> of methiozolin treated roots, and 50 nM is the  $\sim$ GR<sub>80</sub> value of shoots.

<sup>c</sup>Means were separated using Tukey's test, and those followed by the same letter within a column are not significantly different at an alpha of >0.05.

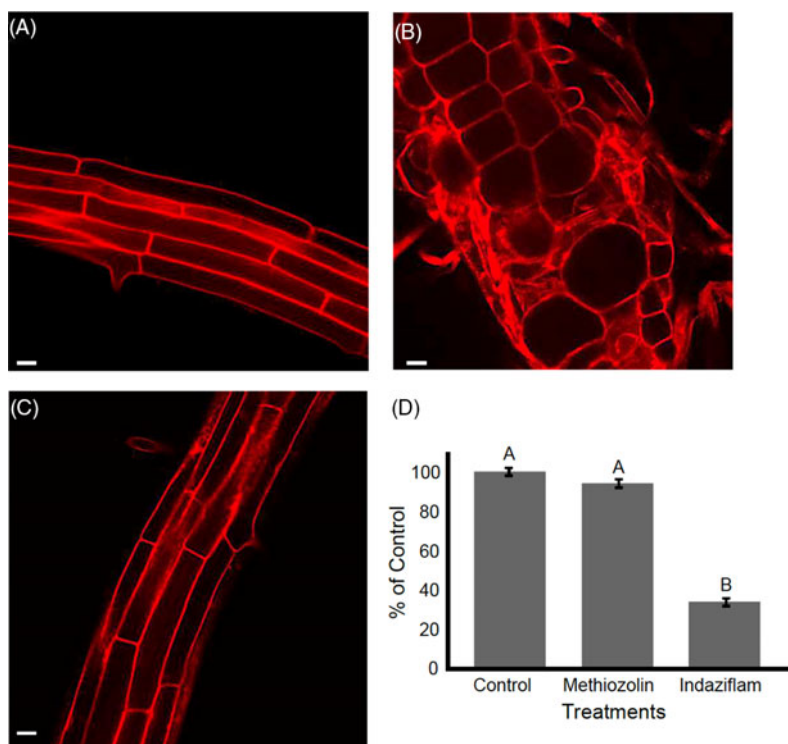


**Figure 2.** Methiozolin effects on *Arabidopsis thaliana* root cell lengths. (A–C). Representative confocal microscopy images of root cell lengths in control and treated transgenic *A. thaliana* plants expressing a red fluorescently labeled aquaporin (plasma membrane intrinsic protein 2) at 3 d after treatment. (A) dimethyl sulfoxide control, (B) 2 nM of a known cellulose biosynthesis inhibitor (indaziflam), (C) and methiozolin at 100 nM (D). Bar chart depicting the mean ( $\pm 1$  standard error) cell length of control and treated plants. In total, 60 cells (6 cells plant<sup>-1</sup>) were measured for each treatment and means were separated using Tukey's test. Different letters between treatments indicate a significant difference at an alpha value of 0.05. Scale bars: 20  $\mu$ m.

supplementing treated *A. thaliana* seedlings with 20  $\mu$ M farnesol or squalene. Lovastatin (1  $\mu$ M) served as a positive control, and this concentration gave symptomologies similar to methiozolin at 50 nM. We expected, at best, farnesol or squalene would partially alleviate the phytotoxicity of lovastatin. This is because several enzymatic steps and important metabolites exist between the biosynthesis of mevalonate and farnesyl diphosphate (farnesol) and subsequently squalene (Vranova et al. 2013). At 7 DAT, lovastatin reduced root length by 88% in comparison to the control (data not shown). The addition of 20  $\mu$ M farnesol, but not squalene, partially (18%) reversed the lovastatin inhibition of root growth. However, the addition of neither farnesol nor squalene could rescue methiozolin-treated plants (data not shown).

### Is Methiozolin an MVA Biosynthesis Inhibitor? Major Phytosterol Measurement

As an alternative approach to test whether methiozolin is an inhibitor of the MVA pathway, we measured phytosterol content in *A. thaliana* seedlings treated with or without methiozolin (1  $\mu$ M) 3 DAT (Figure 4B). Phytosterols are essential components of cell membranes, and the major sterols found in most plants and *A. thaliana* are  $\beta$ -sitosterol, stigmasterol, and the brassinosteroid precursor campesterol (Guo et al. 1995; Hartmann 1998; Schaller 2003). There were no significant differences between treated and untreated seedlings for any of the major sterols measured. Thus, we found no evidence that methiozolin inhibits the MVA pathway, despite the similarities in the symptoms caused by it and the known HMG-CoA reductase inhibitor lovastatin.

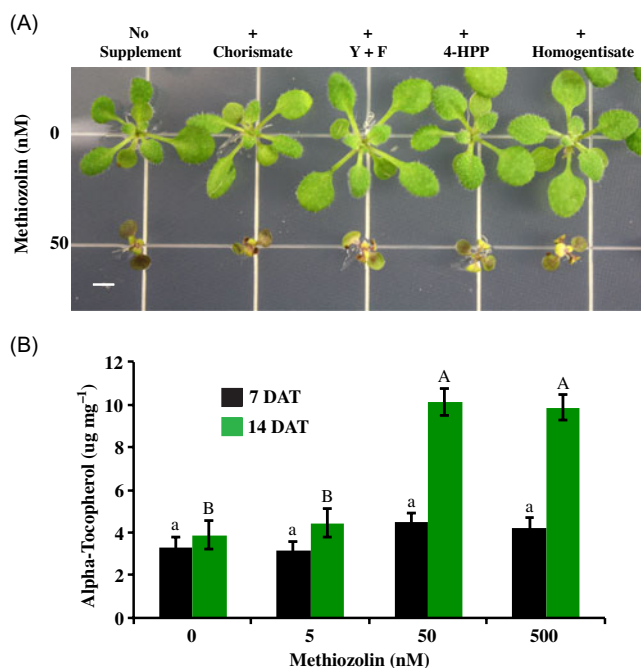


**Figure 3.** Effects of supplements on methiozolin injury to *Arabidopsis thaliana*. (A). Supplements in proposed pathway (chorismate, tyrosine + phenylalanine [Y+F], 4-HPP, and homogentisate at 10  $\mu$ M) did not lessen the phytotoxic effects of 50 nM methiozolin at 14 d after treatment (DAT). Shoots are representatives of the seedlings' response with each combination. (B) Methiozolin, a proposed tocopherol and plastoquinone inhibitor, does not inhibit alpha-tocopherol synthesis at 7 or 14 DAT. Means ( $\pm$  1 standard error) within a time period were separated using Tukey's tests and a different lowercase letter (7 DAT comparisons) or uppercase letter (14 DAT comparisons) indicates a significant difference at an alpha value of 0.05. Scale bar: (A) 0.2 cm.

### Do Methiozolin and Cinnemethylin Result in Similar Physiological Profiles?

Both Grossman et al. (2012) and Campe et al. (2018) described the physiological profile of cinnemethylin phytotoxicity. The primary characteristic of cinnemethylin toxicity is strong growth inhibition in assays with high cell division activity such as *G. mollugo* cell suspension cultures and *L. aequinoctialis*. Growth of photoautotrophic algae and germination of dicotyledonous *L. sativum* seeds were, in contrast, only slightly affected. Comparing the responses to cinnemethylin with those of methiozolin in the same assays (Figure 5), there is a high degree of similarity but with minor differences. Methiozolin showed higher activity on algae and weaker activity on *A. thaliana* than cinnemethylin. Methiozolin also had no activity on CO<sub>2</sub> assimilation and ATP content, while cinnemethylin reduced these slightly (13% to 14%) at the highest concentration (0.1 mM) tested.

### Do Methiozolin and Cinnemethylin Affect FFAs Similarly?

Given the similarities in the physiological profiles between methiozolin and cinnemethylin (Figure 5), we tested whether methiozolin treatment disrupts *A. thaliana* fatty-acid metabolism by examining the change in global fatty-acid composition (14:0 to 26:0) of seedlings treated with methiozolin at 1  $\mu$ M (Figure 6). The fatty-acid levels of 16:1, 16:3, 17:0, 19:0, 20:4, 20:5, 22:5, and 22:6 were less than 1% of the total fatty acids, and 14:0, 14:1, 16:2, 20:3, 22:4, and 26:0 were not detected (data not shown). Otherwise, the fatty-acid profiles of seedlings with or without methiozolin

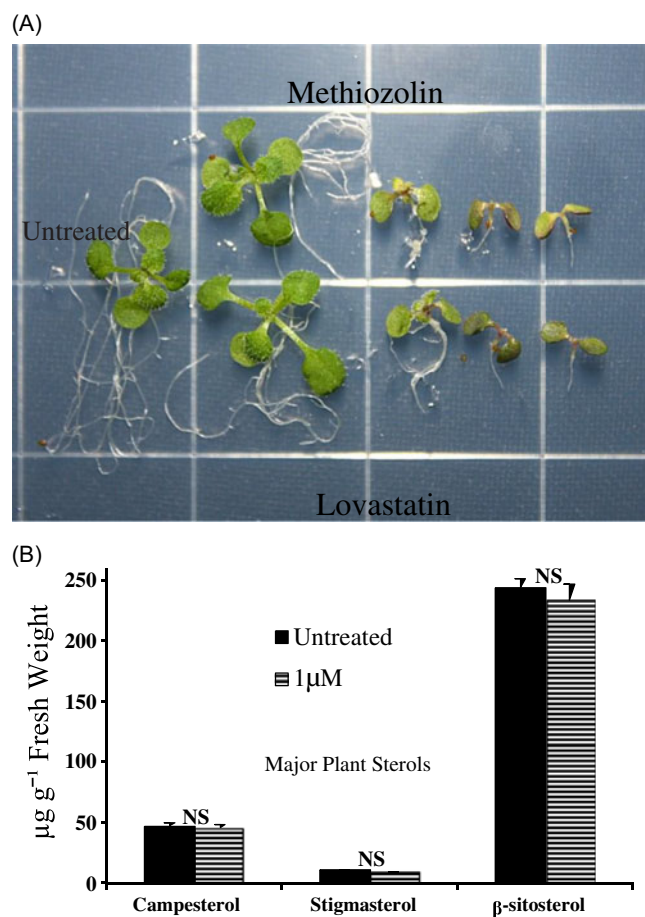


**Figure 4.** Methiozolin was hypothesized to be a mevalonic acid pathway (MVA) inhibitor. (A) The characteristic symptomology of *Arabidopsis thaliana* seedlings treated with increasing rates (left to right) of methiozolin and the MVA inhibitor, lovastatin, at 14 d after treatment (DAT). Notice the rate-dependent similarity between treatments. (B) Comparison of major phytosterol content in *Arabidopsis* seedlings treated with or without methiozolin (1  $\mu$ M) at 3 DAT.

treatment were similar, and no statistical differences existed between any fatty acids from the two treatments. However, the following needs to be considered: (1) the fatty-acid turnover in *A. thaliana* was shown to be extremely low (less than 5% d<sup>-1</sup>; Bao et al. 2000; Bonaventure et al. 2004); (2) the influence of fatty acids derived from seed storage lipids rather than from de novo synthesis in the seedlings was not determined; and (3) the ratio between meristematic and differentiated cells, as well as the low ratio between the levels of FFA versus membrane lipids (Sánchez-Martin et al. 2004), might mask the effects of methiozolin. In addition, even under environmental stress such as drought, the lipid content and class distribution in *A. thaliana* leaves is relatively stable (Gigon et al. 2004). Therefore, we also analyzed the FFA pool after methiozolin treatment. In *Lemna*, we compared the effects of methiozolin with the effects caused by cinnemethylin treatment already described in Campe et al. (2018). Both cinnemethylin and methiozolin reduce C14:0, but the inhibition by cinnemethylin occurs sooner and at a lower concentration (Figure 7). Cinnemethylin affects C16:0 but, in contrast, methiozolin has little effect on C16:0. Both cinnemethylin and methiozolin similarly reduce C18:1 and C18:2, but methiozolin has little effect on C18:3 compared with cinnemethylin. Explaining the observed differences in FFA composition caused by methiozolin and cinnemethylin would be a potential area for further research. Both



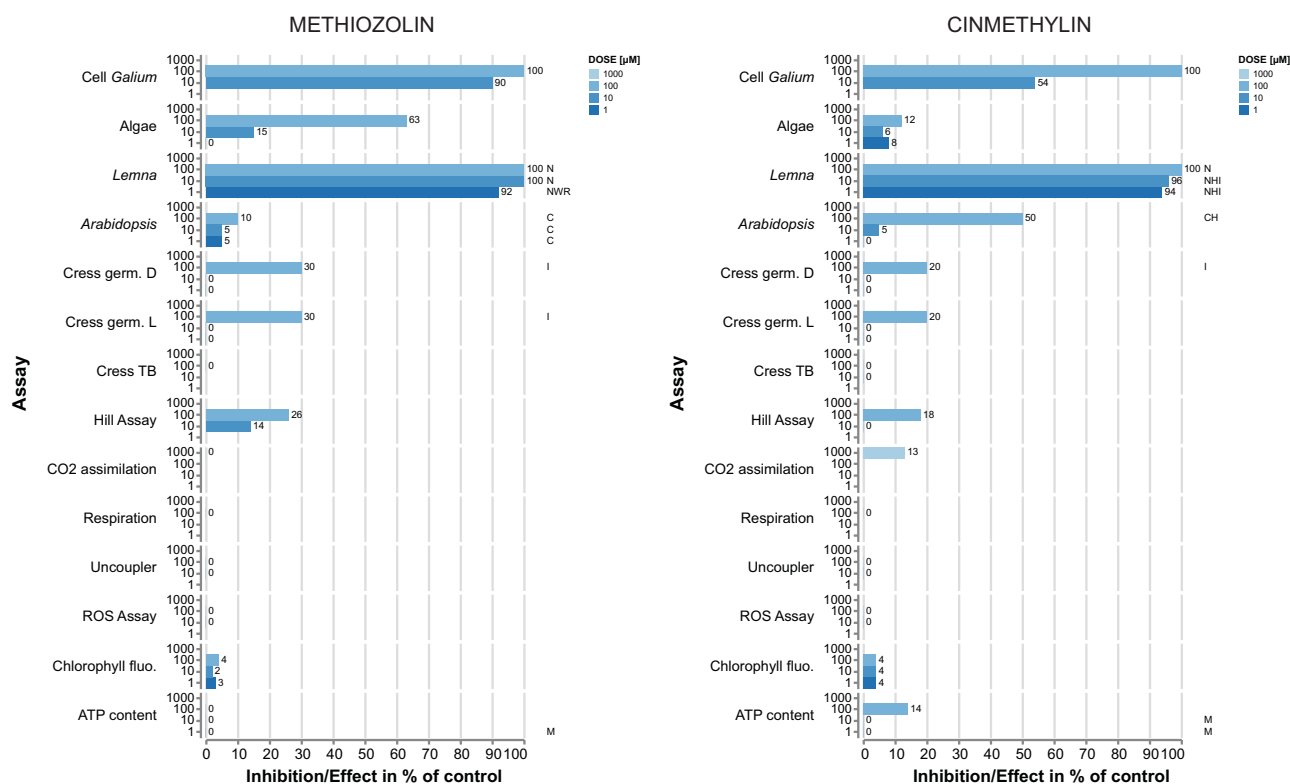


**Figure 5.** Effect of cinmethylin and methiozolin on heterotrophic *Galium mollugo* cell suspensions, green algae *Scenedesmus obliquus*, *Lemna aequinoctialis* plants, *Arabidopsis thaliana* seedling morphology, germination of cress (*Lepidium sativum* L.) under dark/light conditions, toluidine-blue (TB) staining of cress hypocotyls for the detection of inhibition of very-long-chain fatty-acid (VLCFA) synthesis, the Hill reaction in isolated *Triticum aestivum* chloroplasts, CO<sub>2</sub> assimilation in *G. mollugo* plants, oxygen consumption (respiration) in heterotrophic *G. mollugo* cell suspensions, uncoupler activity and accumulation of reactive oxygen species (ROS) in *L. aequinoctialis* root tissue, chlorophyll fluorescence, and ATP content. Uncoupler activity and ROS accumulation are shown as effect compared with control, while values of all other assays are expressed as percentage of inhibition. Letters indicate physiological symptoms observed: necrosis (N), chlorosis (C), reduced leaf growth (H), root growth inhibition (I), intensified leaf pigmentation (WR) and promotive effect (M).

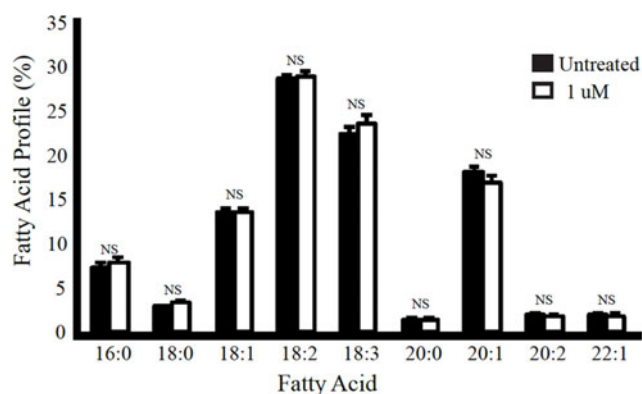


**Figure 6.** The prominent fatty acids of *Arabidopsis thaliana* seedlings untreated or treated with methiozolin at 1 µM. Fatty-acid content is presented as a percentage of the total fatty-acid profile from seedlings within a treatment. The fatty-acid levels of 14:0, 14:1, 16:1, 16:2, 16:3, 17:0, 19:0, 20:3, 20:4, 20:5, 22:4, 22:5, 22:6, and 26:0 were less than 1% of the total fatty-acid profile or not detected. The fatty-acid content was compared with the untreated percentage using Dunnett's test.

cinmethylin and methiozolin show only slight effects on VLCFAs. The effects of methiozolin and cinmethylin on *L. aequinoctialis* FAs are fundamentally different from those caused by ACCase inhibitors and VLCFA inhibitors (Campe et al. 2018).

### Does Methiozolin Bind to FAT?

Campe et al. (2018) used a combination of cellular Target Profiling™, FAT crystallization and cinmethylin binding, and an FTSA to identify FAT enzymes as the target site for cinmethylin binding and inhibition of fatty-acid synthesis. As shown in Figure 8, we determined the melting point for *A. thaliana* FAT A and *L. aequinoctialis* FAT A in the absence and presence of methiozolin. As expected, in the presence of cinmethylin, the melting temperature ( $T_m$ ) of both enzymes significantly increased in the FTSA. Using cinmethylin concentrations between 2.5- to 40-fold of the enzyme concentrations for *A. thaliana* FAT A, the delta  $T_m$  ranged between 6.6 C and 7.6 C, and for *L. aequinoctialis* FAT A between 6.9 C and 7.5 C. Comparably, in the FTSA assay, methiozolin also increased the melting temperature for both the *A. thaliana* and *L. aequinoctialis* FAT A enzymes. Using methiozolin concentrations between 2.5- to 40-fold the enzyme concentrations for *A. thaliana* FAT A, the delta  $T_m$  ranged between 4.5 C to 7.1 C, and for *L. aequinoctialis* FAT A between 5.6 C and 7.4 C. Thus, as with cinmethylin, methiozolin binds to both tested FAT A variants in vitro. Finally, using protein modeling, we compared the binding mode of methiozolin with the cinmethylin binding mode using the *L. aequinoctialis* FAT A-cinmethylin co-crystal structure as a basis (Figure 9). The cinmethylin binding site of FAT A can be divided into three subsites. The first part is a deep hydrophobic pocket (left-hand side in figure), where the *o*-methyltolyl part of cinmethylin binds tightly, forming favorable hydrophobic

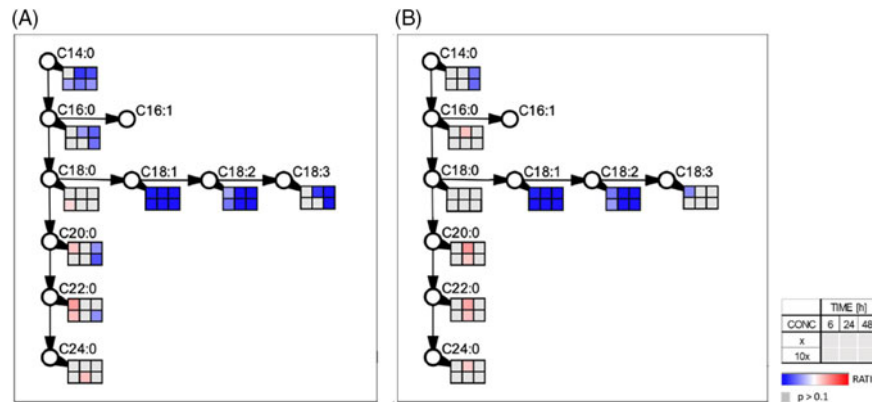


**Figure 7.** Effect of (A) cinmethylin (data published in Campe et al. [2008]) and (B) methiozolin on the composition of free fatty acids (FFAs) in *Lemna aquinoctialis* plants. Boxes indicate accumulation (red) or depletion (blue) of FFAs at three different time points (6, 24, and 48 h after treatment) and two herbicide rates (1 and 10 μM) relative to untreated control. Values were calculated based on three biological replicates.

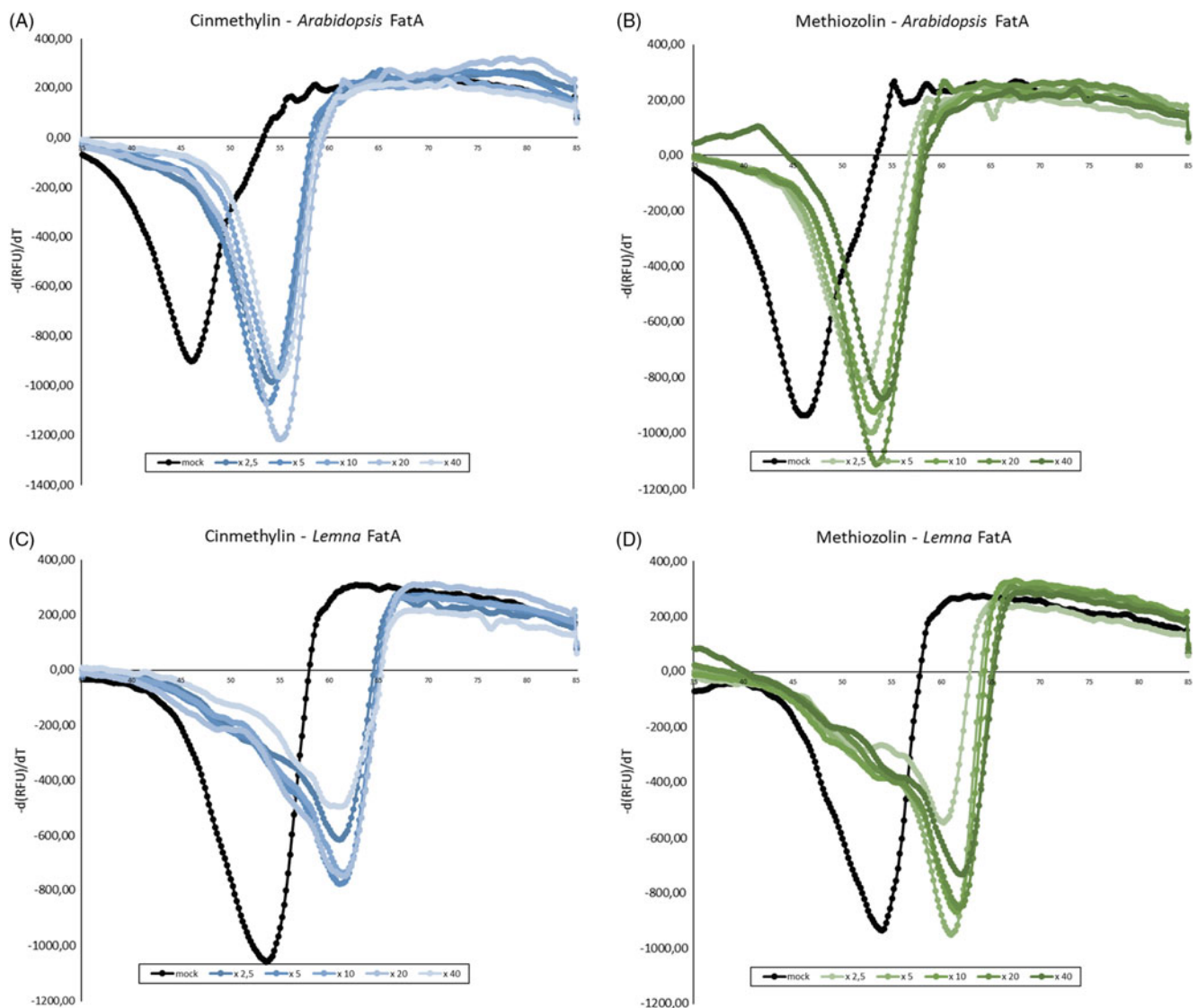


**Figure 8.** Negative first derivatives of relative fluorescence unit (RFU) data over temperature for binding studies of *Arabidopsis thaliana* fatty-acid thioesterase (FAT) A and *Lemna aquinoctialis* FAT A with cinmethylin (blue lines) and methiozolin (green lines) via fluorescence-based thermal shift assay. Functional enzyme concentration was 2.5 μM and inhibitor concentrations of 2.5-, 10-, 20- and 40-fold enzyme concentrations were applied. dimethyl sulfoxide (DMSO) control samples (black lines) show a  $T_m$  value of 47.67 C for *A. thaliana* FAT A and 53.32 for *L. aquinoctialis* FAT A. Upon addition of cinmethylin (A and C) or methiozolin (B and D), considerable shifts in  $T_m$  occurred for both herbicides, indicating binding events. The assay was repeated independently with similar results.

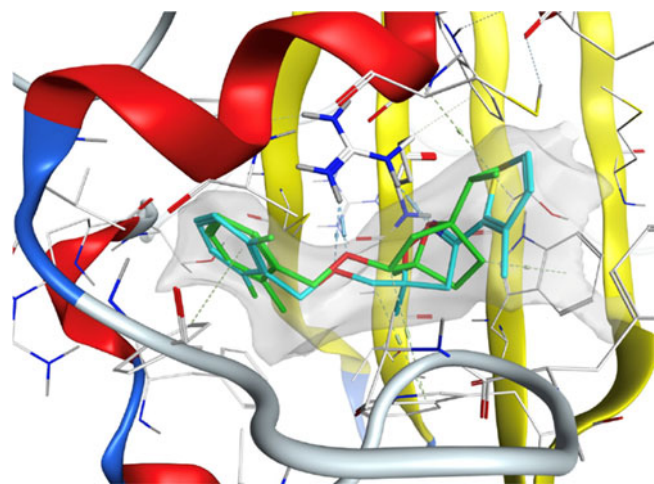


**Figure 9.** In-house X-ray crystal structure of cinmethylin in fatty-acid thioesterase (FAT) A. Cinmethylin is represented as sticks with carbon atoms colored in green and oxygen atoms in red. The protein is shown with secondary structure elements: beta sheets in yellow, alpha-helical structures in red, and loops in blue and gray. Intermolecular interactions are indicated. CH- $\pi$  interactions are highlighted by dotted lines in light green, hydrogen bonds in light blue. Amino acids nearby are shown, with the important arginine in stick representation (white carbons). The proposed binding mode of methiozolin to FAT A is represented as sticks with carbon atoms colored in cyan, oxygen in red, nitrogen in blue, and sulfur in yellow.

contacts, and CH- $\pi$  interactions between the neighboring phenylalanines and a cysteine. In the center, a prominent arginine side chain forms a basic interaction site, where the linker ether oxygen and the oxygen in the bridged ring system of cinmethylin act as hydrogen bond acceptors. Two tryptophan side chains form a hydrophobic cage at the entrance, accommodating the cineol part of cinmethylin. It forms interaction patterns similar to those in the deep site of the pocket. In general, cinmethylin shows several favorable hydrophobic contacts with FAT A and a tight complementary shape fit to the FAT A binding pocket. The binding mode of methiozolin to FAT is very similar to that of cinmethylin. The 2,6-difluorobenzyl binds to the deeper site of the pocket, the ether oxygen and the isoxazole form hydrogen-bonding interactions with the arginine, and the thiophene binds to the hydrophobic entrance of the pocket. Moreover, the thiophene of methiozolin forms a  $\pi$ - $\pi$  stacking with a tryptophan and CH- $\pi$  contact with the backbone of a nearby cysteine.

Methiozolin is an interesting new herbicide with well-documented efficacy on *P. annua* in several warm- and cool-season turfgrasses and with an unknown MOA (Askew and McNulty 2014; Hoisington et al. 2014; Koo et al. 2014; Venner 2015). In this paper, we show methiozolin has activity on the broadleaves *A. thaliana* and soybean (data not shown) in addition to *P. annua* and thus may have broad-spectrum activity. The most characteristic methiozolin symptomatology observed in all species was a cease in meristematic growth. At nonlethal rates, the shoot symptomatology differed between *P. annua* and *A. thaliana*. At 14 DAT, *A. thaliana* was mildly chlorotic (~30% chlorophyll loss) and this, although not quantified, was not obvious in *P. annua*. The *A. thaliana* symptomatology is similar to that described by Grossmann et al. (2012), in which methiozolin-treated (200 nM) *L. aequinoctialis* exhibited photobleaching in newly formed fronds followed by the tissue becoming greenish with a touch of brown and a necrotic meristem.

### Is Methiozolin Activity Dependent on Light or Proliferating Tissue?

Interestingly, we found the activity of methiozolin varied in the presence or absence of light. In the absence of light, it took a nearly 1,000-fold increase in methiozolin rate to have any inhibitory effect on dark-grown etiolated hypocotyls when compared with light-grown roots (Figure 1B and D). Even at our highest tested rate (100  $\mu$ M), hypocotyl length was not reduced by more than 30%. Two major scenarios explain the reduced activity of methiozolin in the dark: (1) light is required for phytotoxicity; or (2) methiozolin has little activity on cells as they elongate, because hypocotyl growth is solely depend on cell elongation and not on cell division (Gendreau et al. 1997). A second point could be that Fatty-acid synthesis is reduced in the dark, and the effect of methiozolin is reduced under this condition. Fatty-acid synthesis is negligible in *A. thaliana* leaves in the dark (Bao et al. 2001).

Our data would indicate the primary methiozolin MOA works on proliferating tissue and does not require light for phytotoxicity. In our CBI MOA experiment, we found methiozolin at 100 nM had little to no effect on the cell length of light-grown PIP2:RFP *A. thaliana* roots at 3 DAT. Other researchers have found methiozolin can significantly reduce *P. annua* panicle number in a dose-dependent manner, but it has only a minor (~20%) effect on panicle length (Askew and McNulty 2014; Koo et al. 2014). However, we cannot exclude the possibility that light may be important for indirect methiozolin phytotoxic effects or could act as a synergist.

### The Inhibitory Mechanism of Methiozolin

Two MOAs were proposed for methiozolin. First, Grossmann and colleagues (2012) followed a logical order of progression from photobleached *L. aequinoctialis* to supplementation with 4-HPP, but not homogentisate, to conclude that methiozolin and related compounds target TATs. Venner (2015) also reported that 4-HPP could slightly (6%) reduce symptoms of methiozolin injury to *L. aequinoctialis*, but it had no effect on methiozolin injury to *P. annua*, *A. stolonifera*, or perennial ryegrass (*Lolium perenne* L.). We also could not rescue methiozolin-treated *A. thaliana* seedlings with supplementation with up- or downstream metabolites to HPPD. In contrast, we could partially rescue mesotrione-treated *A. thaliana* with exogenous homogentisate. In addition, methiozolin did not affect  $\alpha$ -tocopherol levels at 7 DAT, and plants actually had increased  $\alpha$ -tocopherol concentration at 14 DAT. Our data do not support TAT inhibition as an MOA for methiozolin in *A. thaliana*. Later work by Campe et al. (2018) showed that effects on TAT occurred later than other effects for cinmethylin and, presumably, for methiozolin.

Second, Lee et al. (2007) showed decreased  $^{14}$ C-glucose incorporation into cell wall fractions such as cellulose and hemicellulose. However, since the time lag was longer than the growth response, whether methiozolin inhibits cell wall biosynthesis directly remained unknown. Our data show that methiozolin does not directly inhibit cell wall biosynthesis. Analysis of confocal microscopy images of fluorescently labeled *A. thaliana* root cells revealed methiozolin had a negligible effect on cellular anisotropic growth and cell length. Consistent with our results, Venner (2015) found methiozolin did not inhibit the incorporation of [ $^{13}$ C]glucose into cell wall materials of *P. annua*, *A. stolonifera*, *L. perenne*, and Kentucky bluegrass (*Poa pratensis* L.) at 72 h after the beginning of treatment.

During the preparation of this article, another possible MOA for methiozolin appeared in the literature. The MOA of



cinmethylin was recently identified as inhibition of lipid synthesis. Campe et al. (2018) elegantly showed that cinmethylin disrupts cell membranes by preventing the export of saturated and unsaturated C16 or C18 fatty acids from plastids, via FATs, to the endoplasmic reticulum for later incorporation into lipids. Interestingly, Grossman et al. (2012) suggested that methiozolin, cinmethylin, and other 5-benzyloxymethyl-1,2 isoxazolines (ISO1) would share an MOA. This was because they share a 1,4 cineole-like structural motif and have a similar “phytotoxic fingerprint” based on physiological bioassays and metabolomics. It is also clear that the inhibitory mechanism of all these compounds disrupts the ability of meristematic tissue to maintain a proliferative state (Baum et al. 1998; Campe et al. 2018; El-Deek and Hess 1986; Grossmann et al. 2012; Lee et al. 2007). Thus, together with the observed similarities in the extended physiological profile presented here, one could assume the molecular targets of methiozolin are FAT proteins. Even though we found that methiozolin did not quantitatively or qualitatively disrupt global fatty-acid composition at 3 DAT in *A. thaliana*, the FFA profiles after methiozolin or cinmethylin treatment of *L. aequinoctialis* were comparable, supporting FAT enzymes as a common target for both herbicides. Furthermore, using FTSA, we showed that methiozolin binds directly to both *A. thaliana* FAT A and *L. aequinoctialis* FAT A proteins, plus, using the *L. aequinoctialis* FAT A-cinmethylin co-crystal structure as a basis, the protein model suggested a binding mode for methiozolin to FAT A similar to that of cinmethylin. Taken together, the data presented here do not support various physiological processes such as TAT, cellulose synthesis, and chlorophyll biosynthesis as the target site of methiozolin. Instead, they indicate that FAT proteins are the herbicidal targets for methiozolin, and the consequent inhibition of fatty acid synthesis is the MOA for methiozolin. The identical symptomatology of methiozolin and lovastatin was an interesting observation and may warrant further research.

**Supplementary material.** To view supplementary material for this article, please visit <https://doi.org/10.1017/wsc.2020.87>

**Acknowledgments.** This research received no specific grant from any funding agency or the commercial or not-for-profit sectors. No conflicts of interest have been declared.

## References

- Anonymous (2019a) Molecular Operating Environment (MOE). Version 2019.01. Montreal, QC, Canada: Chemical Computing Group
- Anonymous (2019b) U.S. Environmental Protection Agency Registration of PoaCure SC. EPA Registration # 089633-5. [https://www3.epa.gov/pesticides/chem\\_search/ppls/089633-00005-20191209.pdf](https://www3.epa.gov/pesticides/chem_search/ppls/089633-00005-20191209.pdf). Accessed: December 14, 2020
- Askew SD, McNulty BMS (2014) Methiozolin and cumyluron for preemergence annual bluegrass (*Poa annua*) control on creeping bentgrass (*Agrostis stolonifera*) putting greens. *Weed Technol* 28:535–542
- Bao X, Focke M, Pollard M, Ohlrogge J (2000) Understanding in vivo carbon precursor supply for fatty acid synthesis in leaf tissue. *Plant J* 22:39–50
- Baum SF, Karanastasis L, Rost TL (1998) Morphogenetic effect of the herbicide Cinchon on *Arabidopsis thaliana* root development. *J Plant Growth Regul* 14:107–114
- Bonaventure G, Bao X, Ohlrogge J, Pollard M (2004) Metabolic responses to the reduction in palmitate caused by disruption of the FATB gene in *Arabidopsis*. *Plant Physiol* 135:1269–1279
- Brabham C, Debolt S (2012) Chemical genetics to examine cellulose biosynthesis. *Front Plant Sci* 3:309
- Brabham C, Lei L, Gu Y, Stork J, Barrett M, Debolt S (2014) Indaziflam herbicidal action: a potent cellulose biosynthesis inhibitor. *Plant Physiol* 166:1177–1185
- Brosnan JT, Calvache S, Breeden GK, Sorochan, JC (2013) Rooting depth, soil types, and application rate effects on creeping bentgrass injury with amicarbazone and methiozolin. *Crop Sci* 53:655–659
- Campe R, Hollenbach E, Kammerer L, Hendriks J, Hoffken HW, Kraus H, Lerchl J, Mietzner T, Tresch S, Witschel M, Hutzler (2018) A new herbicidal site of action: cinmethylin binds to acyl-ACP thioesterase and inhibits plant fatty acid biosynthesis. *Pest Biochem Phys* 148:116–125
- Cutler SR, Ehrhardt DW, Griffiths JS, Somerville CR (2000) Random GFP: cDNA fusions enable visualization of subcellular structures in cells of *Arabidopsis* at a high frequency. *Proc Natl Acad Sci USA* 97:3718–3723
- DellaPenna D., Pogson BJ (2006) Vitamin synthesis in plants: tocopherols and carotenoids. *Annu Rev Plant Biol* 57:711–738
- El-Deek MH, Hess FD (1986) Inhibited mitotic entry is the cause of growth inhibition by cinmethylin. *Weed Sci* 34:684–688
- Flessner ML, Wehtje GR, McElroy JS (2013) Methiozolin absorption and translocation in annual bluegrass (*Poa annua*). *Weed Sci* 61:201–208
- Gendreau E, Traas J, Desnos T, Grandjean O, Caboche M, Hofte H (1997) Cellular basis of hypocotyl growth in *Arabidopsis thaliana*. *Plant Physiol* 114:295–305
- Gigon A, Matos A-R, Laffray D, Zuily-Fodil Y, Pham-Thi A-T (2004) Effect of drought stress on lipid metabolism in the leaves of *Arabidopsis thaliana* (Ecotype Columbia). *Ann Bot* 94:345–351
- Grossmann K (2005) What it takes to get a herbicide’s mode of action. *Physionomics, a classical approach in a new complexion*. *Pest Manag Sci* 61:423–431
- Grossmann K, Hutzler J, Tresch S, Christiansen N, Looser R, Ehrhardt T (2012) On the mode of action of the herbicides cinmethylin and 5-benzyloxymethyl-1,2-isoxazolines: putative inhibitors of plant tyrosine aminotransferase. *Pest Manag Sci* 68:482–492
- Grossmann K, Niggeweg R, Christiansen N, Looser R, Ehrhardt T (2010) The herbicide saflufenacil (Kixor™) is a new inhibitor of protoporphyrinogen IX oxidase activity. *Weed Sci* 58:1–9
- Guo DA, Venkatramesh M, Nes WD (1995) Developmental regulation of sterol biosynthesis in *Zea mays*. *Lipid* 30:203–209
- Hartmann MA (1998) Plant sterols and the membrane environment. *Trends Plant Sci* 3:170–175
- Hoisington NR, Flessner ML, Schiavon M, McElroy JS, Baird JH (2014) Tolerance of bentgrass (*Agrostis*) species and cultivars to methiozolin. *Weed Technol* 28:501–509
- Holländer-Czytko H, Grabowski J, Sandorf I, Weckermann K, Weiler EW (2005) Tocopherol content and activities of tyrosine aminotransferase and cysteine lyase in *Arabidopsis* under stress conditions. *J Plant Physiol* 162: 767–770
- Huang T, Tohge T, Lytovchenko A, Fernie AR, Jander G (2010) Pleiotropic physiological consequences of feedback-insensitive phenylalanine biosynthesis in *Arabidopsis thaliana*. *Plant J* 63:823–835
- Hwang IT, Kim HR, Jeon DJ, Hong KS, Song JH, Cho KY (2005) 5-(2,6-Difluorobenzyl)oxymethyl-5-methyl-3-(3-methylthiophen-2-yl)-1,2-isoxazoline as a useful rice herbicide. *J Agric Food Chem* 53:8639–8643
- Istvan ES, Deisenhofer J (2001) Structural mechanism for statin inhibition of HMG-CoA Reductase. *Science* 292:1160–1164
- Iverson SJ, Lang SLC, Cooper MH (2001) Comparison of the Bligh and Dyer and Folch methods for total lipid determination in a broad range of marine tissue. *Lipids* 36:1283
- Jiang Z, Kempinski C, Chappell J (2016) Extraction and analysis of terpenes/terpenoids. *Curr Protoc Plant Biol* 1:345–358
- Jones G, Willett P, Glen RC, Leach AR, Taylor R (1997) Development and validation of a genetic algorithm for flexible docking. *J Mol Biol* 267:727–748
- Kobayashi K, Suzuki M, Tang J, Nagata N, Ohyama K, Seki H, Kiuchi R, Kaneko Y, Nakazawa M, Matsui M, Matsumoto S, Yoshida S, Muranaka T (2007) LOVASTATIN INSENSITIVE 1, a novel pentatricopeptide repeat protein, is a potential regulatory factor of isoprenoid biosynthesis in *Arabidopsis*. *Plant Cell Physiol* 48:322–331
- Koo SJ, Hwang KH, Jeon MS, Kim SH, Lim J, Lee DG, Cho NG (2014) Methiozolin [5-(2,6-difluorobenzyl)oxymethyl-5-methyl-3,3(3-methylthiophen-2-yl)-1,2-isoxazoline], a new annual bluegrass (*Poa annua* L.) herbicide for turfgrasses. *Pest Manag Sci* 70:156–162

- Layton CJ, Hellinga HW (2010) Thermodynamic analysis of ligand-induced changes in protein thermal unfolding applied to high-throughput determination of ligand affinities with extrinsic fluorescent dyes. *Biochemistry* 49: 10831–10841
- Lee JN, Koo SJ, Hwang KH, Hwang IT, Jeon DJ, Kim, HR (2007) Mode of action of a new isoxazoline compound. Pages 597–601 in Proceedings of the 21st Asian Pacific Weed Science Society Conference. Colombo, Sri Lanka: Asian Pacific Weed Science Society
- McCullough PE, Barreda DG, Yu J (2013) Selectivity of methiozolin for annual bluegrass (*Poa annua*) control in creeping bentgrass as influenced by temperature and application timing. *Weed Sci* 61:209–216
- Porfirova S, Bergmuller E, Tropf S, Lemke R, Dormann P (2002) Isolation of an *Arabidopsis* mutant lacking vitamin E and identification of a cyclase essential for all tocopherol biosynthesis *Proc Natl Acad Sci USA* 99: 12495–12500
- Riewe D, Koohi M, Lisek J, Pfeiffer M, Lippman R, Schmeichel J, Willmitzer L, Altmann T (2012) A tyrosine aminotransferase involved in tocopherol synthesis in *Arabidopsis*. *Plant J* 71:850–859
- Ritchie RJ (2006) Consistent sets of spectrophotometric chlorophyll equations for acetone, methanol and ethanol solvents. *Photosynth Res* 89:27–41
- Ritz C, Baty F, Streibig JC, Gerhand D (2015) Dose-response analysis using R. *PLoS ONE* 10: e01460251
- Rodríguez-Concepcion M, Fores O, Martinex-Garcia JF, Gonzalez V, Phillipis M, Ferrer A, Boronat A (2004) Distinct-light-mediated pathways regulate the biosynthesis and exchange of isoprenoid precursors during *Arabidopsis* seedling development. *Plant Cell* 16:144–156
- Ryu EK, Kim HR, Jeon DJ, Song JW, Kim KM, Lee JN, Kim HC, Hong SH, inventors; Korea Research Institute of Chemical Technology, assignee (2002) September 7. Preparation of herbicidal 5-benzoxymethyl-1,2-isoxazoline derivatives of weed control in rice. US patent WO200209185
- Sabba RP, Vaughn KC (1999) Herbicides that inhibit cellulose biosynthesis. *Weed Sci* 47:757–763
- Sánchez-Martín J, Canales FJ, Tweed JKS, Lee MRF, Rubiales D, Gómez-Cadenas A, Arbona V, Mur LAJ, Prats E (2004) Fatty acid profile changes during gradual soil water depletion in oats suggests a role for jasmonates in coping with drought. *Front Plant Sci* 9:1077
- Schaller H (2003) The role of sterols in plant growth and development. *Prog Lipid Res* 42:163–175
- Schneider CA, Rasband WS, Eliceiri KW (2012) NIH Image to ImageJ: 25 years of image analysis. *Nature Methods* 9:671–675
- Shaner DL, ed (2014) *Herbicide Handbook*. 10th ed. Lawrence, KS: Weed Science Society of America. Pp 12, 413
- Soto G, Stritzler M, Lisi C, Alleva K, Pagano ME, Ardila F, Mozzicafreddo M, Cuccioloni M, Angeletti M, Ayub ND (2011) Acetoacetyl-CoA thiolase regulates the mevalonate pathway during abiotic stress adaptation. *J Exp Bot* 62:5699–711
- Suzuki M, Kamide Y, Nagata N, Seki H, Ohyama K, Kato H, Masuda K, Sato S, Kato T, Tabata S, Yoshida S, Muranaka T (2004) Loss of function of 3-hydroxy-3-methylglutaryl coenzyme A reductase 1 (HMG1) in *Arabidopsis* leads to dwarfing, early senescence and male sterility, and reduced sterol levels. *Plant J* 37:750–761
- Venner KA (2015) Evaluating Methiozolin Programs for Golf Putting Greens and Investigating Potential Modes of Action. Ph.D dissertation. Blackburg, VA: Virginia Tech. 165 p
- Vranova E, Coman D, Groussin W (2013) Network analysis of the MVA and MEP pathways for isoprenoid synthesis. *Annu Rev Plant Biol* 64:665–700
- Xu Z (2002) Analysis of tocopherols and tocotrienols. *Curr Protoc Food Anal Chem* 4:D1.5.1-D1.5.1.2
- Yu J, McCullough PE (2014) Methiozolin efficacy, absorption, and fate in six cool-season grasses. *Crop Sci* 54:1211–1219